

## Electronic Supplementary Information for

# Highly Efficient Synthesis of Zeolite Chabazite using Cooperative Hydration-Mismatched Inorganic Structure-Directing Agents

*Adam J. Mallette<sup>1</sup>, Gabriel Espindola<sup>1</sup>, Nathan Varghese<sup>1</sup>, Jeffrey D. Rimer<sup>1,\*</sup>*

<sup>1</sup>*Chemical and Biomolecular Engineering, University of Houston, Houston, TX 77204, USA*

\*Correspondence sent to: [jrimer@central.uh.edu](mailto:jrimer@central.uh.edu)

### Table of Contents

Experimental.....	2
Supporting Figures.....	4
Supporting Tables.....	14
References.....	19

### List of Figures

1. Low-temperature Na-zeolite phase diagram
2. K-zeolite phase diagrams
3. Medium and high temperature Na,Li-zeolite phase diagrams
4. Low and medium temperature Li phase diagrams with specific dense phases
5. Lithium silicate phase formation in Na,Li synthesis before crystallization
6. PXRD patterns for varying Li/(Na+Li)
7. PXRD pattern of FAU synthesized using aluminum hydroxide
8. PXRD patterns of syntheses with binary ISDAs
9. PXRD patterns for mixtures of kosmotrope and chaotrope cations
10. PXRD patterns used to estimate induction and total crystallization times of CHA products
11. PXRD pattern peak shifts for zeolite samples
12. Time-resolved ICP analysis of lithium concentration in solids
13. Relationship between ionic radius and crystallization kinetics
14. Selected SEM images

### List of Tables

1. Synthesis details of ABW syntheses from literature used to generate Figure 1c
2. Synthesis details of sodium syntheses from literature used to generate Figure S1
3. Synthesis details of sodium (90%) lithium (10%) syntheses used to generate Figure 1a
4. Synthesis details of potassium (90%) lithium (10%) syntheses used to generate Figure 1b
5. Synthesis details of lithium syntheses used to generate Figure 1d

## Experimental

### Materials

LUDOX AS-40 colloidal silica ( $\text{SiO}_2$ , Sigma Aldrich, 40 wt% suspension), aluminum hydroxide ( $\text{Al}(\text{OH})_3$ , Sigma Aldrich, >99.9%), lithium hydroxide ( $\text{LiOH}$ , Alfa Aesar, 98% anhydrous powder), sodium hydroxide ( $\text{NaOH}$ , Sigma Aldrich, 98% anhydrous pellets), potassium hydroxide ( $\text{KOH}$ , Sigma Aldrich, 85% pellets), strontium hydroxide octahydrate ( $\text{Sr}(\text{OH})_2 \cdot 8\text{H}_2\text{O}$ , Alfa Aesar, 99% crystalline powder), and cesium hydroxide ( $\text{CsOH}$ , Alfa Aesar, 50 wt% aqueous solution) were used as received. Deionized (DI) water used for all syntheses was filtered with an Aqua Solutions RODI-C-12A purification system (18.2 M $\Omega$ ).

### Zeolite Synthesis

*Syntheses for pure lithium phase diagram.* Zeolite growth mixtures were prepared with molar compositions of  $x \text{SiO}_2:y \text{Al}_2\text{O}_3:5 \text{Li}_2\text{O}:600 \text{H}_2\text{O}$  by mixing aluminum hydroxide and lithium hydroxide into DI water. These solutions were stirred for 5 min until visually well mixed. LUDOX AS-40 was then added as the silica source. Growth mixtures were stirred at room temperature for 24 h, then heated for 7 days in a convection oven (Thermo Fisher) at 65, 100, or 160 °C in polypropylene bottles (for the 65 and 100 °C conditions) or Teflon-lined stainless-steel autoclaves (for the 160 °C condition).

*Syntheses of sodium-lithium and potassium-lithium phase diagrams.* Zeolite growth mixtures containing sodium and lithium were prepared with molar compositions of  $x \text{SiO}_2:y \text{Al}_2\text{O}_3:1 \text{Li}_2\text{O}:4 \text{Na}_2\text{O}:600 \text{H}_2\text{O}$  following the same protocols reported above for pure lithium syntheses, with the exception of a high temperature of 180 °C instead of 160 °C. Zeolite growth mixtures containing potassium and lithium were prepared with molar compositions of  $x \text{SiO}_2:y \text{Al}_2\text{O}_3:0.5 \text{Li}_2\text{O}:4.5 \text{K}_2\text{O}:600 \text{H}_2\text{O}$  following the same preparation reported above. These synthesis mixtures were then heated in polypropylene bottles for 7 days at 85 °C. Values of  $x$  range from 0.75 – 15 and values of  $y$  range from 0.3 – 13.

*Optimized CHA synthesis.* Growth mixtures for zeolite chabazite (CHA) were prepared with molar compositions of  $4.76 \text{SiO}_2:0.56 \text{Al}_2\text{O}_3:x \text{SrO}:y \text{M}_2\text{O}:z \text{H}_2\text{O}$  where  $M$  represents the alkali metals ( $\text{Li}^+$ ,  $\text{Na}^+$ ,  $\text{K}^+$ , and  $\text{Cs}^+$ ), which were present in molar ratios  $y = 0 - 5$ , where the sum for all cations combined was 5. The molar ratio of SrO ( $x$ ) was either 0 or 0.24; and the molar ratio of  $\text{H}_2\text{O}$  ( $z$ ) was varied from 150 to 600. Each growth mixture was prepared by first adding metal hydroxide(s) to DI water in a polypropylene bottle (60 mL) and stirring with a magnetic stir bar for 5 min or until fully dissolved. Aluminum hydroxide was then added to the bottle and stirred for 5 min. Finally, colloidal silica (LUDOX AS-40) was added to the growth mixture using a plastic pipette. After colloidal silica was added, the growth mixture was stirred for 24 h at room temperature in a polypropylene bottle. After this aging period, the magnetic stir bar was removed from the growth mixture, and the polypropylene bottle was transferred to a ThermoFisher Precision oven preheated to 85 °C. Samples were removed from the oven and quenched in a water bath at room temperature after a set heating period (0 – 19 days). Solids were recovered using three cycles of centrifugation and washing with DI water. Each centrifugation cycle was performed for 5 min at 5 °C using a Beckman Coulter Avanti J-E centrifuge rotating at 13,000 rpm. Recovered solids were dried in petri dishes overnight in an oven at 55 °C.

*Synthesis of Na,K,Cs-CHA adapted from Mintova and coworkers.<sup>1</sup>* Zeolite growth mixtures containing sodium, potassium, and cesium were prepared with molar compositions of  $4.76 \text{SiO}_2:0.56 \text{Al}_2\text{O}_3:3.9 \text{Na}_2\text{O}:1.0 \text{K}_2\text{O}:0.1 \text{Cs}_2\text{O}:600 \text{H}_2\text{O}$  following the same protocols reported above for pure lithium syntheses. These synthesis mixtures were then heated in polypropylene bottles for 7 days at 85 °C.

### Material Characterization

Powder X-ray diffraction (PXRD) patterns were collected on a Rigaku diffractometer using  $\text{Cu K}\alpha$  radiation (40 kV, 40 mA). Data were collected with a step size of  $0.02^\circ$  ( $2\theta$ ) at a rate of 8.33 steps per second. Fractions of crystalline phases were calculated by measuring their peak area using Rigaku PDXL Software.

The quantity of stacking faults was calculated according to the method established by Kim and Kim<sup>2</sup> for CHA zeolites by comparing the ratio of PXRD peak heights at 7.4° and 9.7°. Scanning electron microscopy (SEM) was conducted on a FEI-235 Dual-Beam Focused Ion Beam instrument operated at 15 kV and a 5 mm working distance. Samples for SEM analysis were prepared by affixing dried crystals to a SEM sample holder with carbon tape. Electron dispersive spectroscopy (EDS) was performed with a FEI 235 dual-beam (focused ion beam) system operated at 12 kV and a 15 mm working distance. Textural analysis and BET surface area estimation was made from N<sub>2</sub> adsorption/desorption data collected with a Micromeritics 3Flex instrument; and micropore volume was determined from the t-plot method. Molar ratios of solid zeolite samples were measured by inductively-coupled plasma with optical emission spectroscopy (ICP-OES). Before analysis, a Katanax X-300 Fusion Fluxer instrument was used to conduct the fusion of samples (approximately 50 mg) prepared by first dissolving with LiBO<sub>2</sub> (98.5 wt% lithium metaborate and 1.5 wt% LiBr). The mixture was heated to 1000°C for 15 min, then 2 N HNO<sub>3</sub> (50 mL) was added to the molten mixture and stirred for 10 min. The elemental components of the samples were analyzed using an Agilent 725 instrument.

## Supporting Figures

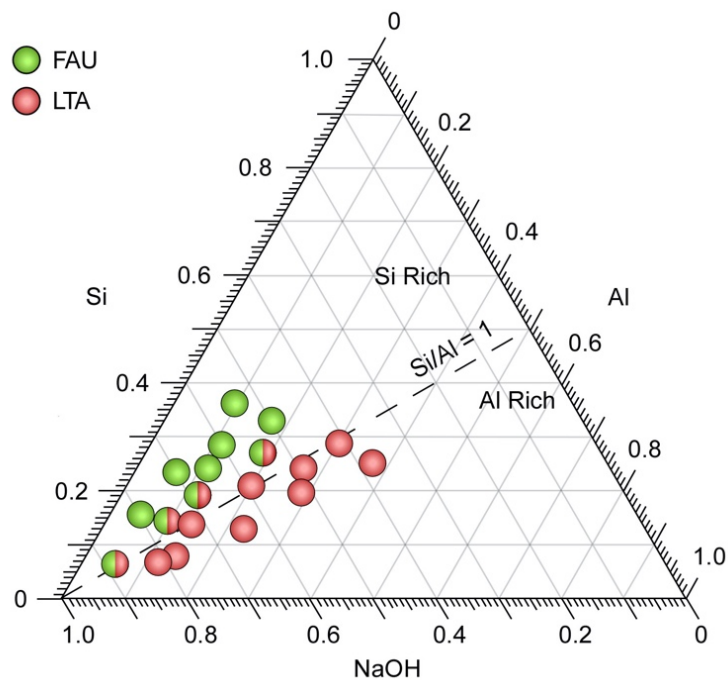


**Figure S1.** Ternary kinetic phase diagram for 7-day zeolite syntheses at 65 °C using Na<sup>+</sup> as the only ISDA. The conditions for each data point are listed in Table S2. This diagram was reproduced using data from ref. <sup>3</sup>

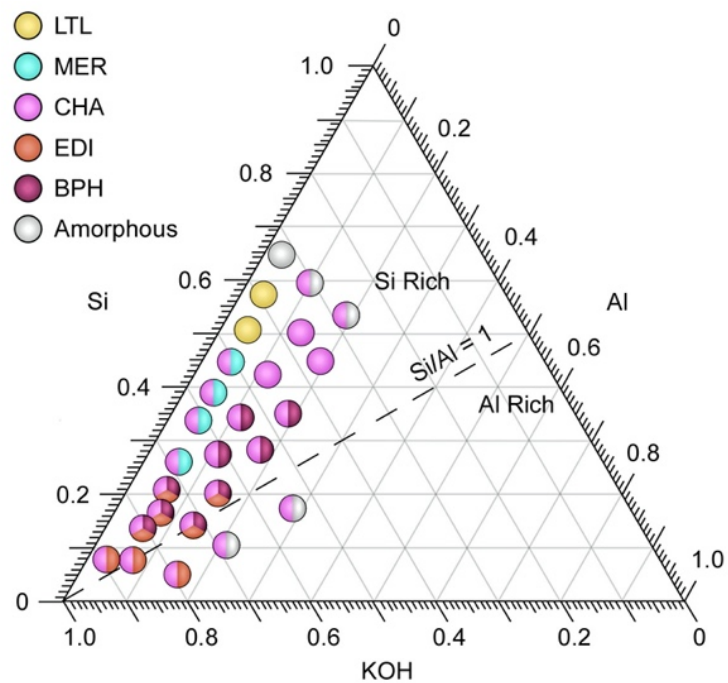


**Figure S2.** Kinetic ternary phase diagram for syntheses conducted at 85 °C for 21 days using K<sup>+</sup> as the sole ISDA. The phase diagram was reproduced using data from ref. <sup>4</sup>.

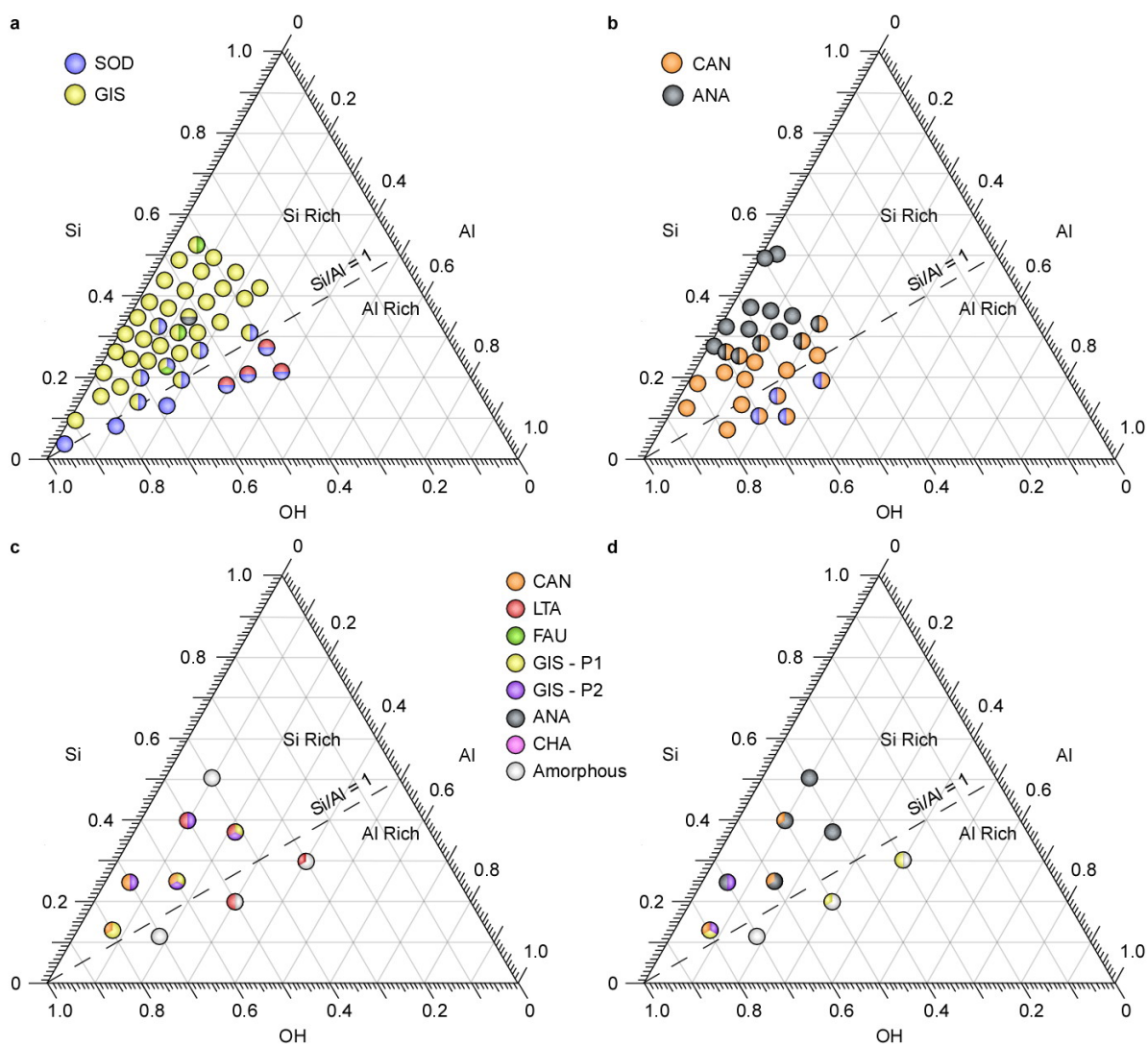


**Figure S3.** Kinetic ternary phase diagrams for zeolite syntheses at (a,c) 100 °C and (b,d) 180 °C. The diagrams refer to syntheses using (a,b)  $\text{Na}^+$  as the only ISDA (reproduced from data in ref. <sup>3</sup>) and (c,d) mixtures of  $\text{Na}^+$  and  $\text{Li}^+$  at a molar ratio of 4:1. Growth mixtures with a molar composition of  $x$  Si: $y$  Al:11 NaOH:190  $\text{H}_2\text{O}$  were treated for (a) 7 days and (b) 21 days using LUDOX AS-40, sodium aluminate, and sodium hydroxide reagents. (c, d) Growth mixtures with a molar composition of  $x$  Si: $y$  Al:8 NaOH:2 LiOH:600  $\text{H}_2\text{O}$  were treated for 7 days using LUDOX AS-40, aluminum hydroxide, sodium hydroxide, and lithium hydroxide reagents.

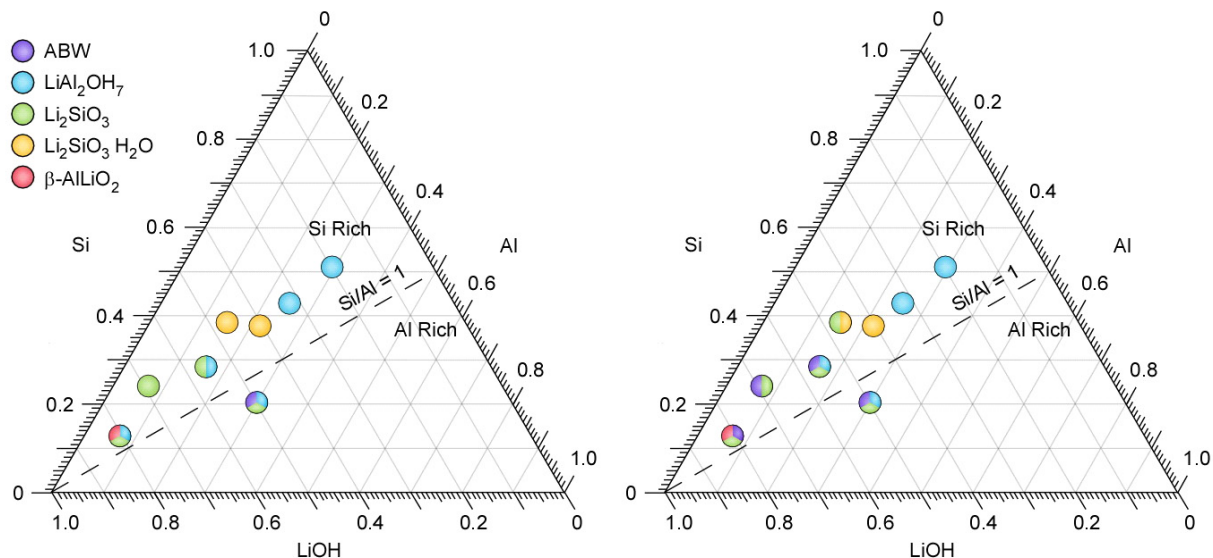


**Figure S4.** Kinetic ternary phase diagrams for syntheses at (left) 85 °C and (right) 120 °C using  $\text{Li}^+$  as the sole ISDA. Growth mixtures with a molar composition of  $x$  Si: $y$  Al:10 LiOH:600  $\text{H}_2\text{O}$  were treated for 7 days using LUDOX AS-40, aluminum hydroxide, and lithium hydroxide reagents.

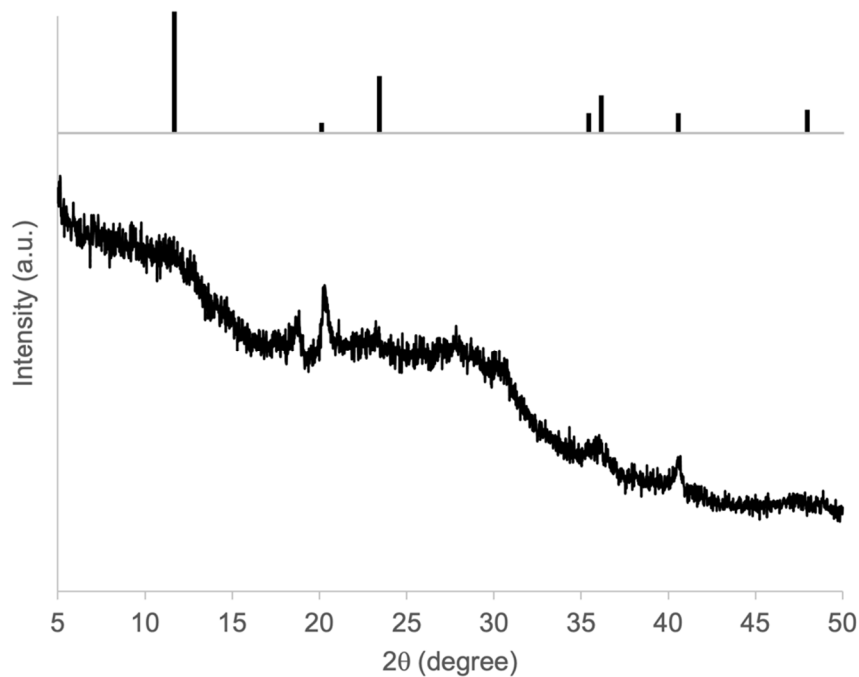


**Figure S5.** PXRD pattern of the solids extracted from a growth mixture with a molar composition of 4.76 Si:1.11 Al:8 NaOH:2 LiOH:600  $\text{H}_2\text{O}$  after 1 day of heating at 85 °C. The pattern reveals evidence of a lithium aluminum hydroxide phase that forms prior to zeolite crystallization in syntheses using a mixture of  $\text{Na}^+$  and  $\text{Li}^+$  as ISDAs. The reference pattern (top) for  $\text{LiAl}_2(\text{OH})_7 \cdot 2\text{H}_2\text{O}$  was obtained from ref. <sup>5</sup>.

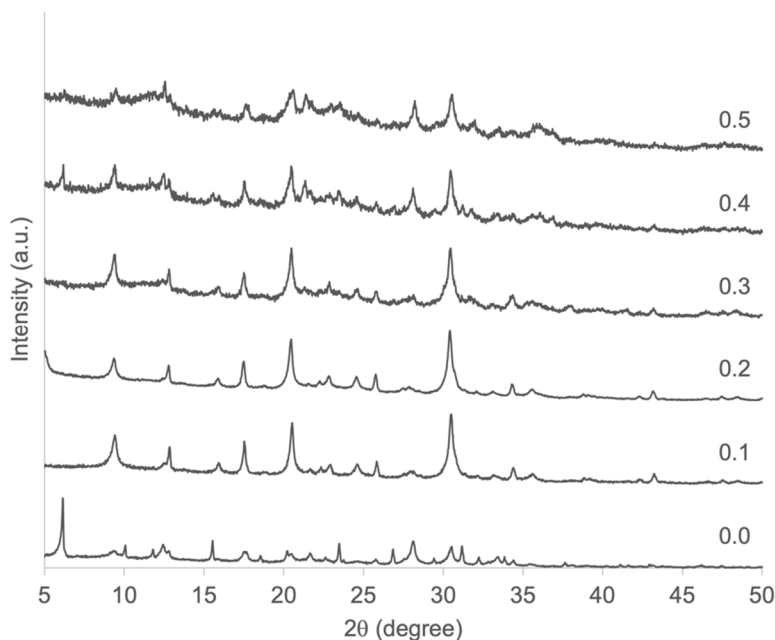


**Figure S6.** PXRD patterns for syntheses where the Li/(Na+Li) molar ratio is varied (as labelled). The molar compositions of growth mixtures are  $4.76 \text{ SiO}_2:0.56 \text{ Al}_2\text{O}_3:x \text{ Na}_2\text{O}:y \text{ Li}_2\text{O}:600 \text{ H}_2\text{O}$  where  $(x + y) = 5$ . Samples were heated for 7 days at  $85^\circ\text{C}$ . The percentage of phases calculated based on peak area were used to generate Figure 3a.

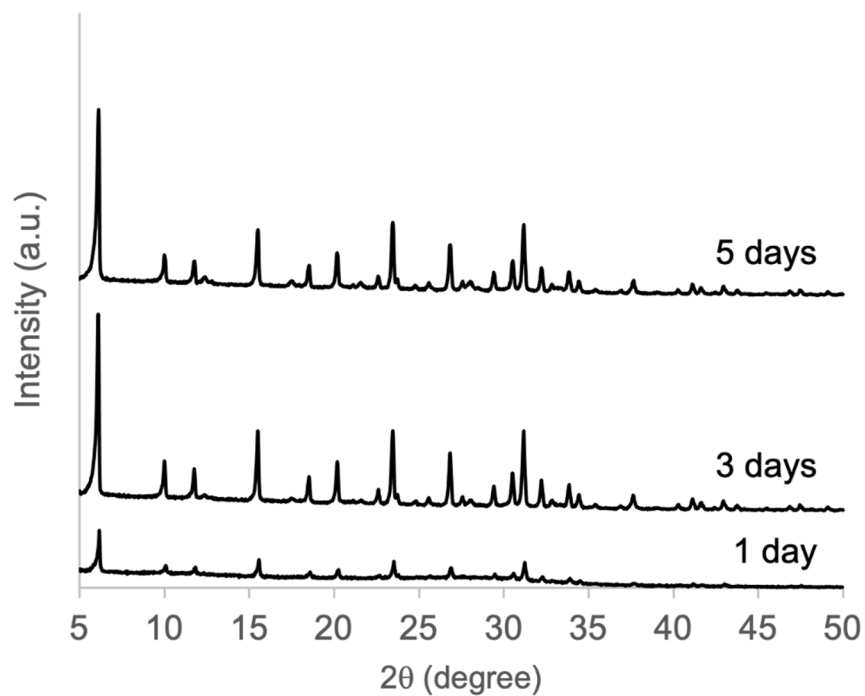


**Figure S7.** PXRD patterns for syntheses of zeolite FAU using a molar ratio of  $4.76 \text{ SiO}_2:0.56 \text{ Al}_2\text{O}_3:5 \text{ Na}_2\text{O}:600 \text{ H}_2\text{O}$  heated for different times at  $85^\circ\text{C}$  using  $\text{Al}(\text{OH})_3$  as the aluminum source.

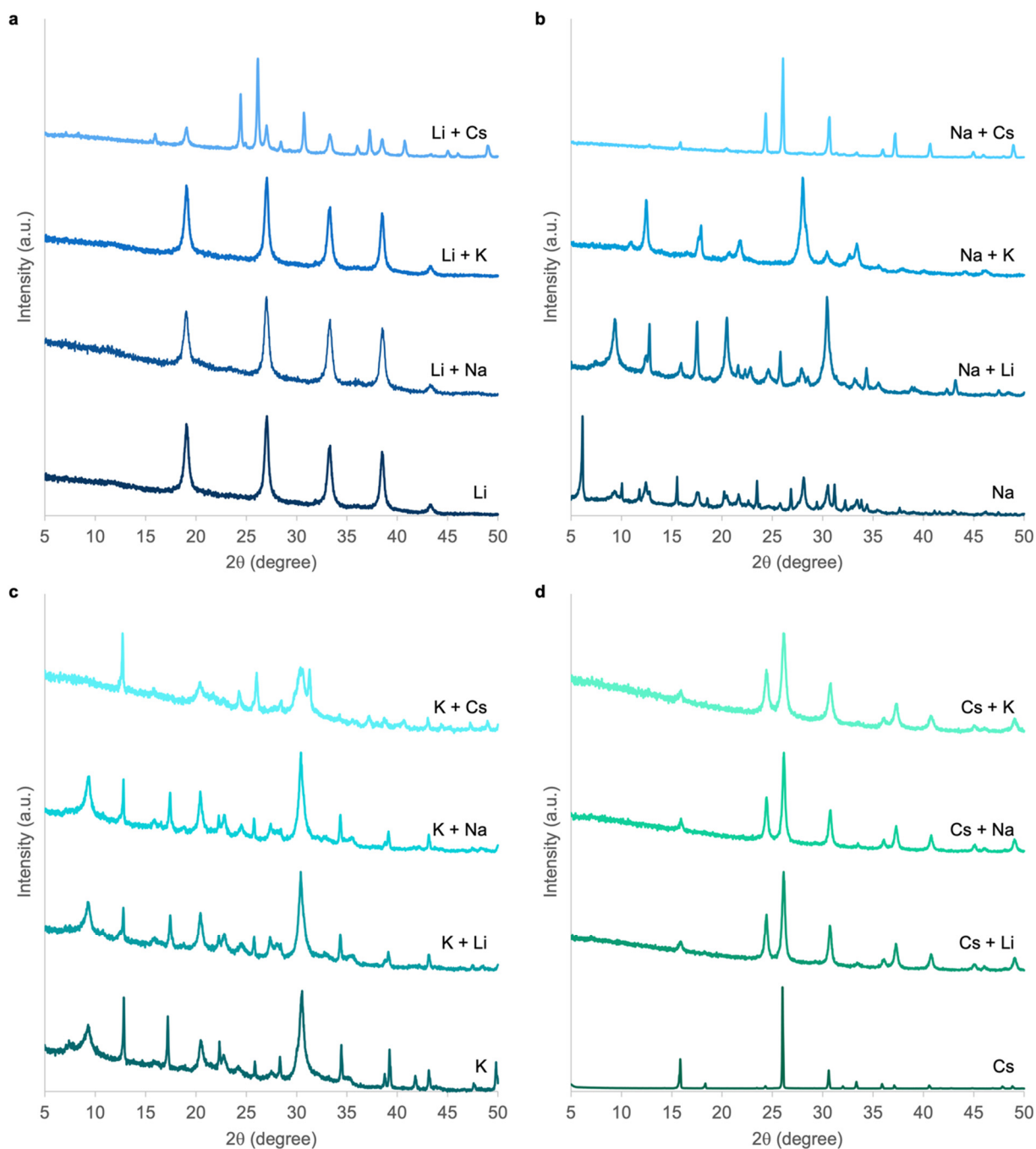


**Figure S8.** PXRD patterns of crystalline products reported in Figure 3 that were synthesized using binary combinations of cations where (a) Li, (b) Na, (c) K, and (d) Cs are the major elements used in each synthesis mixture. The molar compositions of growth mixtures are  $4.76 \text{ SiO}_2:0.56 \text{ Al}_2\text{O}_3:4.5 \text{ Q}_2\text{O}:0.5 \text{ W}_2\text{O}:600 \text{ H}_2\text{O}$  where  $Q$  and  $W$  are major and minor cation components, respectively. Samples were heated for 7 days at  $85^\circ\text{C}$ .



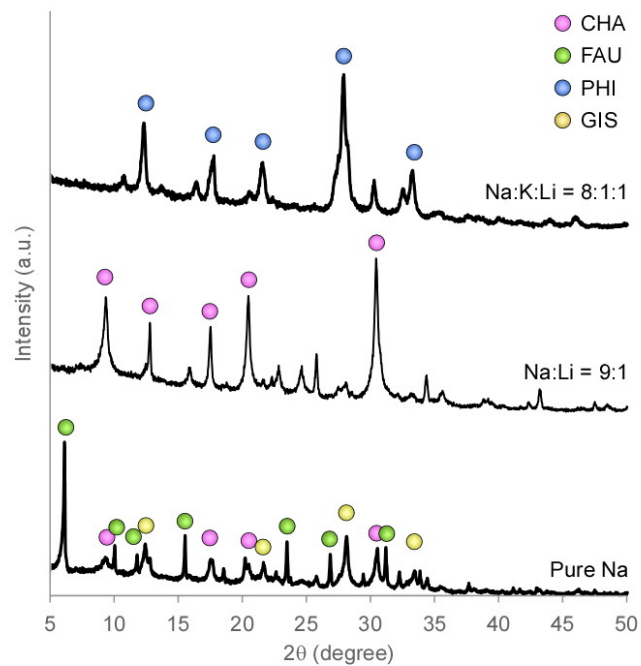


**Figure S9.** PXRD patterns of solids collected from growth mixtures heated at 65 °C for 7 days in the presence of different mixtures of inorganic cations. The molar compositions of growth mixtures are 4.76 SiO<sub>2</sub>:0.56 Al<sub>2</sub>O<sub>3</sub>:5 M<sub>2</sub>O:600 H<sub>2</sub>O where M represents the combination of all alkali metals.

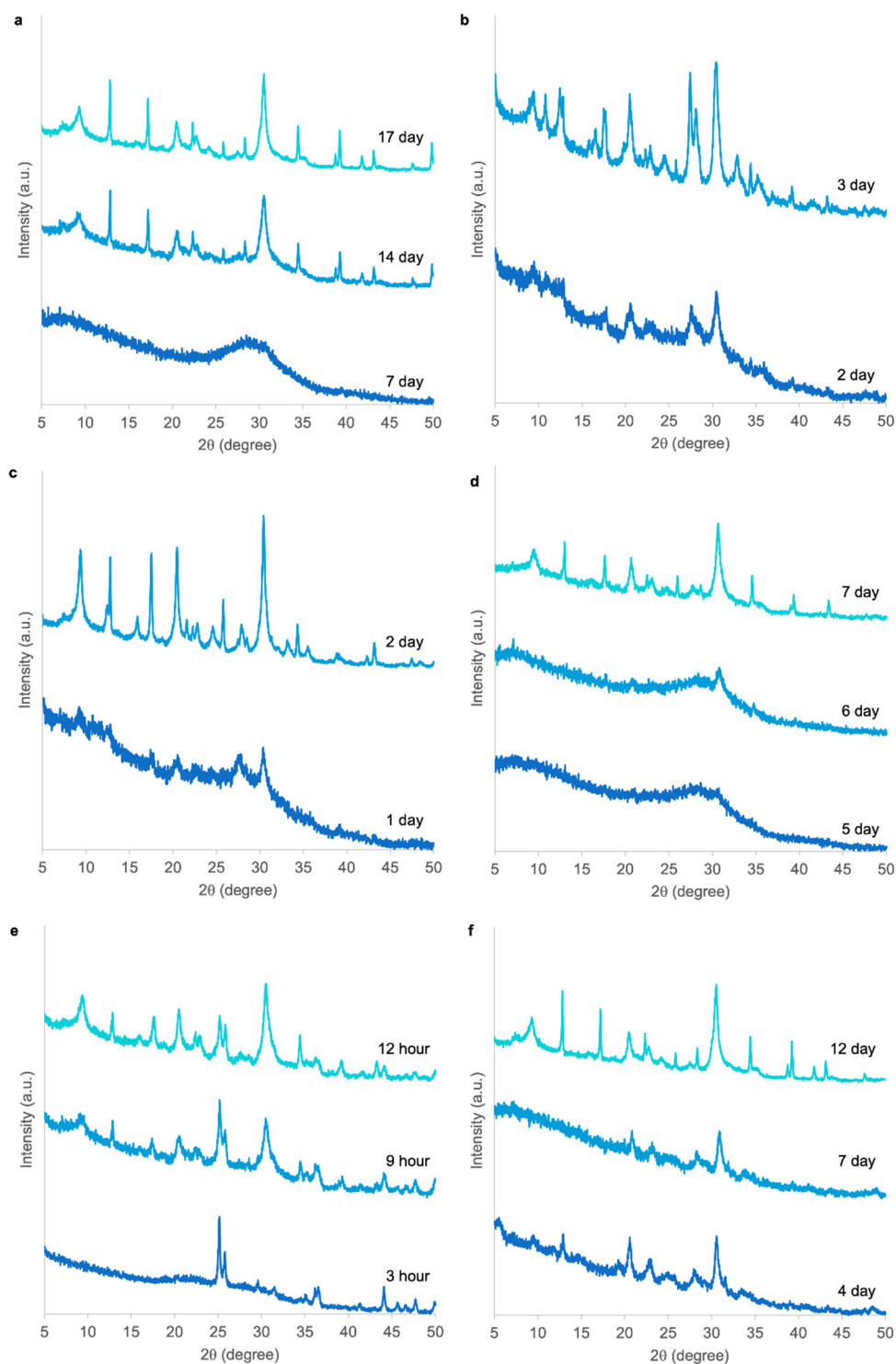


**Figure S10.** PXRD patterns used to estimate the induction and total crystallization times of zeolite CCHA products reported in Figure 4. These samples were synthesized using (a)  $\text{K}^+$ , (b)  $\text{K}^+$  and  $\text{Li}^+$ , (c)  $\text{Na}^+$  and  $\text{Li}^+$ , (d)  $\text{K}^+$  and  $\text{Na}^+$ , (e)  $\text{K}^+$  and  $\text{Sr}^{2+}$ , and (f)  $\text{Na}^+$ ,  $\text{K}^+$ , and  $\text{Cs}^+$ . The molar compositions of growth mixtures are  $4.76 \text{ SiO}_2:0.56 \text{ Al}_2\text{O}_3:4.5 \text{ Q}_2\text{O}:0.5 \text{ W}_2\text{O}:600 \text{ H}_2\text{O}$  where  $Q$  and  $W$  are major and minor cation components, respectively, except when  $W = \text{Sr}$ , where the molar ratio is 0.24 instead of 0.5, and when a ternary combination of cations is used, where the molar ratio of cations is  $3.9 \text{ Na}_2\text{O}:1.0 \text{ K}_2\text{O}:0.1 \text{ Cs}_2\text{O}$ . All samples were heated at  $85^\circ\text{C}$ .

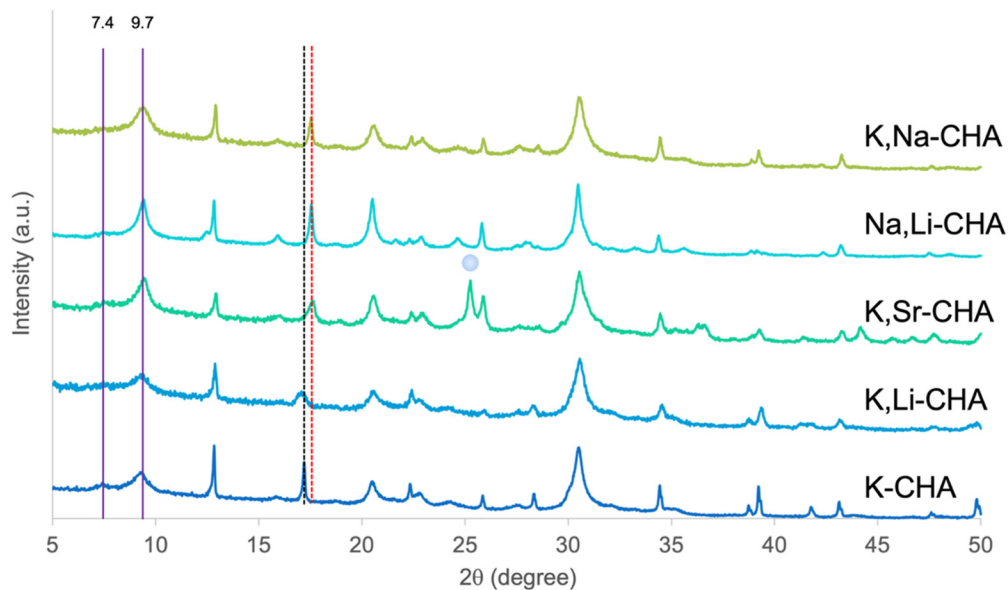


**Figure S11.** PXRD patterns of zeolite CHA samples illustrating a peak shift near  $2\theta = 17.8^\circ$  for sodium-containing samples (red dashed line) relative to those without sodium (black dashed line). The circle at  $\sim 25^\circ$  for the K,Sr-CHA sample indicates a peak from a  $\text{Sr}(\text{OH})_2$  impurity phase. Peaks at  $7.4^\circ$  and  $9.7^\circ$  (purple lines) were used to calculate the percentage of stacking faults (see Methods).

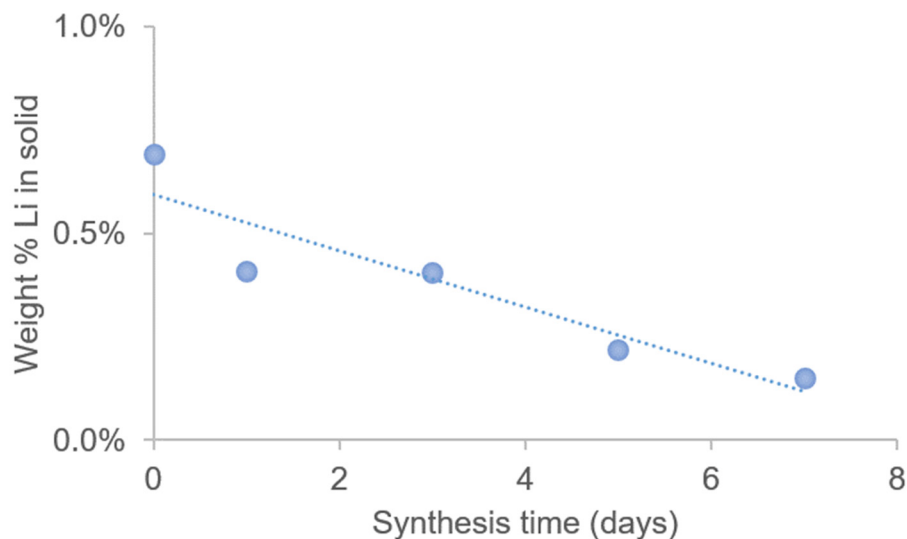


**Figure S12.** Weight percent of lithium in solids (solid circles) collected from a Na,Li-CHA growth mixture heated at  $85^\circ\text{C}$  for different times. The elemental composition of solids was analyzed using ICP. The dashed line is interpolated as a guide to the eye.

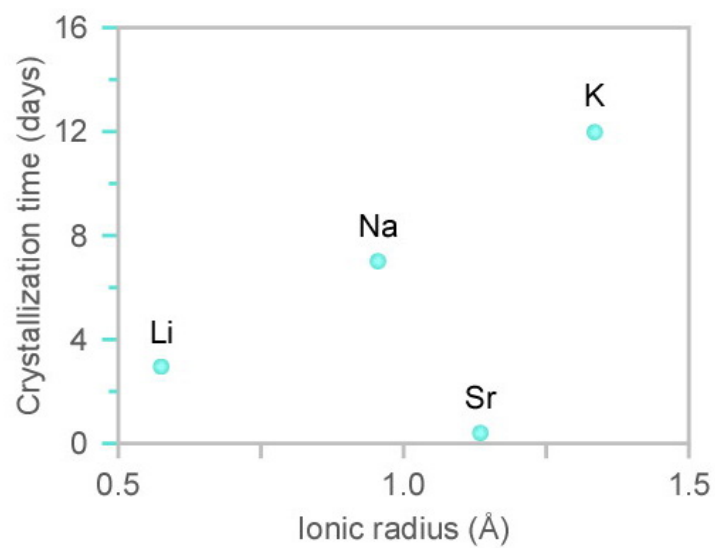


**Figure S13.** Correlation between (anhydrous) ionic radius size and zeolite CHA crystallization kinetics when  $K^+$  in the synthesis mixture is partially replaced with the elements indicated above each data point.

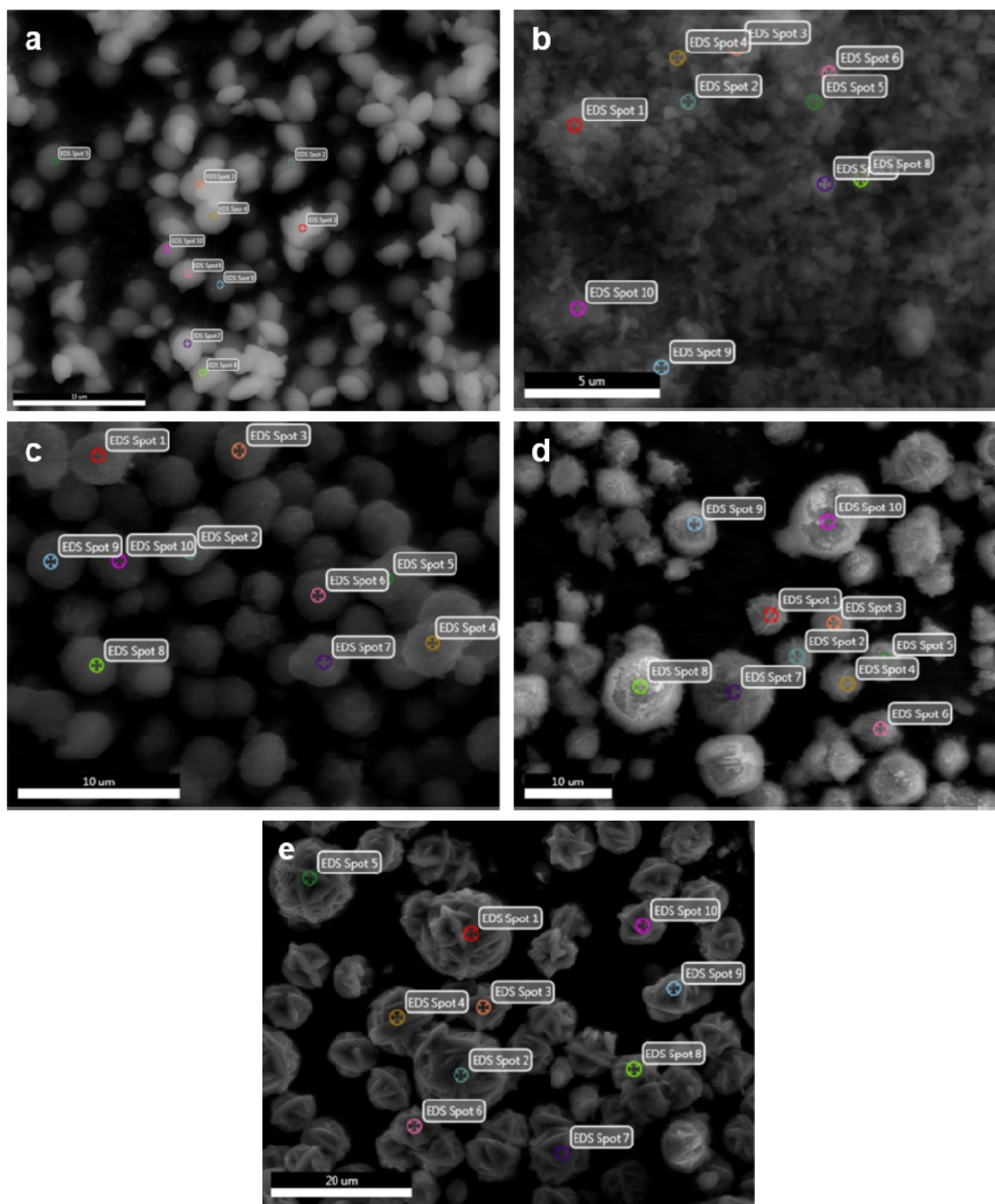


**Figure S14.** Scanning electron micrographs of zeolite CHA crystals synthesized using (a)  $K^+$  and  $Li^+$ , (b)  $K^+$  and  $Sr^{2+}$ , (c)  $Na^+$  and  $Li^+$ , (d)  $K^+$  and  $Na^+$ , and (e)  $K^+$  and ISDAs. Refer to the caption of Figure S8 for details of the synthesis conditions. Syntheses of zeolite CHA resulted in polydisperse size distributions for the majority of alkali and alkaline earth cation combinations.

## Supporting Tables

**Table S1.** Reported syntheses of ABW from literature depicted in Figure 1c

Ref.	Temperature (°C)	Synthesis Time	Si	Al	OH	Cation	Product
6	90	24 days	0.20	0.20	0.60	Li	ABW + EDI
	90	24 days	0.22	0.22	0.56	Li	ABW + EDI
	100	24 days	0.20	0.20	0.60	Li	ABW + EDI
	100	1 day	0.22	0.22	0.56	Li	EDI (ABW)
	100	5 days	0.22	0.22	0.56	Li	EDI (ABW)
	100	8 days	0.22	0.22	0.56	Li	ABW + EDI
	100	16 days	0.22	0.22	0.56	Li	ABW + EDI
	100	24 days	0.22	0.22	0.56	Li	ABW + EDI
	100	24 days	0.25	0.25	0.50	Li	ABW + EDI
7	175	7 days	0.16	0.16	0.68	Li	ABW
8	200	4 days	0.36	0.36	0.27	Li	ABW
9	200	1 day	0.18	0.18	0.64	0.4 Na, 0.6 Tl	ABW
	200	1 day	0.18	0.18	0.64	0.4 K, 0.6 Tl	ABW
	200	1 day	0.18	0.18	0.64	0.4 Li, 0.6 Tl	ABW
10	180	12 hours	0.37	0.31	0.31	Li	ABW
11	250	4 days	0.16	0.16	0.68	Li	ABW
12	150	7 days	0.29	0.29	0.43	Li	ABW
	100	7 days	0.29	0.29	0.43	Li	ABW + amorph
	120	7 days	0.29	0.29	0.43	Li	ABW + amorph
	150	7 days	0.29	0.29	0.43	Li	ABW
	180	7 days	0.29	0.29	0.43	Li	ABW
	150	7 days	0.33	0.33	0.33	Li	ABW
	150	7 days	0.25	0.25	0.50	Li	ABW + amorph
	150	7 days	0.22	0.22	0.56	Li	ABW + Li <sub>2</sub> SiO <sub>3</sub>
	13	180	4 hours	0.11	0.05	0.84	Cs
14	180	2 hours	0.11	0.05	0.84	Cs	ABW
	180	80 mins	0.13	0.07	0.80	Cs	ABW
	180	80 mins	0.11	0.05	0.84	Cs	ABW
	180	80 mins	0.11	0.05	0.84	Cs	ABW
	180	80 mins	0.11	0.05	0.84	Cs	ABW
	180	80 mins	0.11	0.05	0.84	Cs	ABW
	180	80 mins	0.06	0.06	0.89	Cs	ABW
	180	80 mins	0.15	0.05	0.80	Cs	ABW
	180	1 hour	0.11	0.05	0.84	Cs	ABW + amorph
15	180	2 hours	0.11	0.05	0.84	Cs	ABW
	150	1 day	0.27	0.13	0.60	Li	ABW

**Table S2.** Synthesis compositions for mixtures presented in Figure S1.

<b>Si</b>	<b>Al</b>	<b>NaOH</b>	<b>Product</b>
0.05	0.05	0.90	FAU
0.06	0.12	0.82	FAU
0.07	0.14	0.79	FAU
0.13	0.13	0.73	FAU
0.14	0.09	0.77	FAU
0.15	0.04	0.81	FAU
0.19	0.13	0.69	FAU + LTA
0.23	0.06	0.71	FAU + LTA
0.20	0.20	0.60	FAU + LTA
0.24	0.12	0.65	FAU + LTA
0.19	0.29	0.52	LTA
0.13	0.23	0.64	LTA
0.28	0.11	0.61	LTA
0.24	0.27	0.49	LTA
0.27	0.18	0.54	LTA
0.33	0.17	0.50	LTA
0.25	0.38	0.38	LTA
0.28	0.31	0.41	LTA
0.36	0.09	0.55	LTA
0.05	0.05	0.90	FAU
0.06	0.12	0.82	FAU

All samples were aged at room temperature for 24 h and heated for 7 days at 65 °C. The overall molar composition for all synthesis mixtures is  $x$  SiO<sub>2</sub>: $y$  Al<sub>2</sub>O<sub>3</sub>:5.5 Na<sub>2</sub>O:190 H<sub>2</sub>O. Data was obtained from ref. <sup>3</sup>

**Table S3.** Synthesis compositions for mixtures presented in Figure 1a.

<b>Si</b>	<b>Al</b>	<b>(Na+Li)OH</b>	<b>Product</b>
0.50	0.10	0.40	Amorphous
0.38	0.20	0.42	Amorphous
0.13	0.17	0.70	Amorphous
0.40	0.10	0.50	Amorphous + LTA
0.30	0.40	0.30	Amorphous + LTA
0.20	0.30	0.50	Amorphous + LTA
0.37	0.03	0.60	Amorphous + CHA
0.24	0.11	0.55	Amorphous + CHA
0.30	0.19	0.51	Amorphous + CHA
0.25	0.10	0.65	Amorphous + CHA
0.20	0.03	0.67	FAU
0.34	0.02	0.64	Amorphous + CHA + FAU
0.20	0.04	0.76	Amorphous + CHA + FAU
0.28	0.02	0.70	Amorphous + CHA + GIS
0.20	0.12	0.68	Amorphous + CHA + GIS
0.24	0.05	0.71	CHA + GIS
0.25	0.15	0.60	FAU + GIS
0.14	0.06	0.80	FAU + GIS
0.30	0.06	0.64	CHA
0.33	0.07	0.60	CHA
0.30	0.10	0.60	CHA

All samples were aged at room temperature for 24 h and heated for 7 days at 65 °C. The overall molar composition for all synthesis mixtures is  $x$  SiO<sub>2</sub>: $y$  Al<sub>2</sub>O<sub>3</sub>:4 Na<sub>2</sub>O:1 Li<sub>2</sub>O:600 H<sub>2</sub>O.



**Table S4.** Synthesis compositions for mixtures presented in Figure 1b.

<b>Si</b>	<b>Al</b>	<b>(K+Li)OH</b>	<b>Product</b>
0.47	0.07	0.46	LTL
0.50	0.10	0.40	Amorphous + LTL
0.40	0.10	0.50	MER
0.30	0.08	0.92	MER + CHA
0.27	0.03	0.70	MER + CHA
0.20	0.02	0.78	MER + CHA
0.19	0.12	0.69	CHA
0.16	0.14	0.69	CHA
0.10	0.10	0.80	CHA
0.15	0.20	0.65	CHA
0.35	0.15	0.50	Amorphous + CHA
0.30	0.50	0.20	Amorphous + CHA
0.28	0.12	0.60	Amorphous + CHA
0.25	0.16	0.59	Amorphous + CHA
0.20	0.20	0.60	Amorphous + CHA
0.17	0.23	0.60	Amorphous + CHA
0.20	0.10	0.70	Amorphous + CHA
0.13	0.17	0.60	Amorphous + CHA
0.10	0.15	0.75	Amorphous + CHA
0.06	0.14	0.80	Amorphous + CHA
0.07	0.08	0.85	Amorphous + CHA
0.07	0.03	0.90	Amorphous
0.15	0.05	0.80	Amorphous
0.22	0.29	0.49	Amorphous
0.25	0.25	0.50	Amorphous
0.43	0.14	0.43	Amorphous
0.44	0.20	0.36	Amorphous
0.49	0.16	0.35	Amorphous
0.55	0.12	0.33	Amorphous
0.58	0.03	0.39	Amorphous

All samples were aged at room temperature for 24 h and heated for 7 days at 85 °C. The molar composition for all synthesis mixtures is  $x$  SiO<sub>2</sub>: $y$  Al<sub>2</sub>O<sub>3</sub>:4 K<sub>2</sub>O:1 Li<sub>2</sub>O:600 H<sub>2</sub>O.

**Table S5.** Synthesis compositions for mixtures presented in Figure 1d.

Si	Al	LiOH	H <sub>2</sub> O/Li <sub>2</sub> O	Product
0.50	0.30	0.20	120	LiAl <sub>2</sub> (OH) <sub>7</sub>
0.40	0.40	0.20	120	LiAl <sub>2</sub> (OH) <sub>7</sub>
0.42	0.25	0.33	120	Li <sub>2</sub> SiO <sub>3</sub> H <sub>2</sub> O
0.38	0.22	0.40	120	Li-ABW + Li <sub>2</sub> SiO <sub>3</sub>
0.38	0.15	0.47	120	Li-ABW + Li <sub>2</sub> SiO <sub>3</sub>
0.28	0.16	0.56	120	Li-ABW + Li <sub>2</sub> SiO <sub>3</sub>
0.24	0.69	0.07	120	Li-ABW + Li <sub>2</sub> SiO <sub>3</sub>
0.27	0.48	0.25	120	Li-ABW
0.26	0.30	0.44	120	Li-ABW
0.20	0.36	0.44	120	Li-ABW
0.19	0.43	0.38	120	Li-ABW
0.14	0.36	0.50	120	Li-ABW
0.20	0.30	0.50	120	Li-ABW
0.15	0.30	0.55	120	Li-ABW
0.21	0.24	0.55	120	Li-ABW
0.08	0.42	0.50	120	Li <sub>2</sub> SiO <sub>3</sub> H <sub>2</sub> O + Li <sub>2</sub> SiO <sub>3</sub>
0.08	0.29	0.63	120	Li <sub>2</sub> SiO <sub>3</sub> H <sub>2</sub> O + β-AlliO <sub>2</sub>
0.05	0.05	0.90	120	Li <sub>2</sub> SiO <sub>3</sub> H <sub>2</sub> O + β-AlliO <sub>2</sub>
0.15	0.15	0.70	120	Li-ABW + Li <sub>2</sub> SiO <sub>3</sub> H <sub>2</sub> O + β-AlliO <sub>2</sub>
0.13	0.07	0.80	120	Li <sub>2</sub> SiO <sub>3</sub> + β-AlliO <sub>2</sub>

All samples were aged at room temperature for 24 h and treated hydrothermally for 7 days at 160 °C. The overall molar composition for all synthesis mixtures is  $x$  SiO<sub>2</sub>: $y$  Al<sub>2</sub>O<sub>3</sub>:5 Li<sub>2</sub>O:600 H<sub>2</sub>O.

## References

1. Ghojavand, S., E.B. Clatworthy, A. Vicente, E. Dib, V. Ruaux, M. Debost, J. El Fallah, and S. Mintova, *The role of mixed alkali metal cations on the formation of nanosized CHA zeolite from colloidal precursor suspension*. Journal of Colloid and Interface Science, 2021. **604**: p. 350-357.
2. Kim, J. and D.H. Kim, *Synthesis of faulted CHA-type zeolites with controllable faulting probability*. Microporous and Mesoporous Materials, 2018. **256**: p. 266-274.
3. Maldonado, M., M.D. Oleksiak, S. Chinta, and J.D. Rimer, *Controlling crystal polymorphism in organic-free synthesis of Na-zeolites*. Journal of the American Chemical Society, 2013. **135**(7): p. 2641-2652.
4. Chawla, A., A.J. Mallette, R. Jain, N. Le, F.C.R. Hernández, and J.D. Rimer, *Crystallization of potassium-zeolites in organic-free media*. Microporous and Mesoporous Materials, 2022. **341**: p. 112026.
5. Thiel, J.P., C.K. Chiang, and K.R. Poeppelmeier, *Structure of lithium aluminum hydroxide dihydrate (LiAl<sub>2</sub>(OH)<sub>7</sub>·2H<sub>2</sub>O)*. Chemistry of Materials, 1993. **5**(3): p. 297-304.
6. Matsumoto, T., T. Miyazaki, and Y. Goto, *Synthesis and characterization of Li-type EDI zeolite*. Journal of the European Ceramic Society, 2006. **26**(4-5): p. 455-458.
7. Bellussi, G., G. Perego, A. Carati, U. Cornaro, and V. Fattore, *5-1 SBU Based Zeolites from Wholly Inorganic Systems*, in *Studies in Surface Science and Catalysis*. 1988, Elsevier. p. 37-44.
8. Lin, D.-C., X.-W. Xu, F. Zuo, and Y.-C. Long, *Crystallization of JBW, CAN, SOD and ABW type zeolite from transformation of meta-kaolin*. Microporous and Mesoporous Materials, 2004. **70**(1-3): p. 63-70.
9. Andersen, I.G.K., E.K. Andersen, P. Norby, C. Colella, and M. de'Gennaro, *Synthesis and structure of an ABW type thallium aluminosilicate*. Zeolites, 1991. **11**(2): p. 149-154.
10. Yao, Z.T., M.S. Xia, Y. Ye, and L. Zhang, *Synthesis of zeolite Li-ABW from fly ash by fusion method*. Journal of Hazardous Materials, 2009. **170**(2-3): p. 639-644.
11. Robson, H., *Verified synthesis of zeolitic materials*. 2001: Gulf Professional Publishing.
12. Liu, G., Q. Shi, L. Liu, H. Xu, J. Li, and J. Dong, *Synthesis and characterization of zeolite Li-ABW from Li<sub>2</sub>O-Al<sub>2</sub>O<sub>3</sub>-SiO<sub>2</sub>-H<sub>2</sub>O*, in *Studies in Surface Science and Catalysis*. 2008, Elsevier. p. 185-188.
13. Ghrear, T.M.A., E.-P. Ng, C. Vaultot, T.J. Daou, T.C. Ling, S.H. Tan, B.S. Ooi, and S. Mintova, *Recyclable synthesis of Cs-ABW zeolite nanocrystals from non-reacted mother liquors with excellent catalytic henry reaction performance*. Journal of Environmental Chemical Engineering, 2020. **8**(1): p. 103579.
14. Ghrear, T.M.A., S. Rigolet, T.J. Daou, S. Mintova, T.C. Ling, S.H. Tan, and E.-P. Ng, *Synthesis of Cs-ABW nanozeolite in organotemplate-free system*. Microporous and Mesoporous Materials, 2019. **277**: p. 78-83.
15. Chen, Y.-C., D.-Y. Lin, and B.-H. Chen, *Transesterification of acid soybean oil for biodiesel production using lithium metasilicate catalyst prepared from diatomite*. Journal of the Taiwan Institute of Chemical Engineers, 2017. **79**: p. 31-36.